LANGMUIR

pubs.acs.org/Langmuir Article

Davydov Split Aggregates of Cyanine Dyes on Self-Assembled Nanotubes

Nitin Ramesh Reddy, Samuel Rhodes, Yiping Ma, and Jiyu Fang*

Cite This: *Langmuir* 2020, 36, 13649−13655 Read Online

ACCESS | Metrics & More | Article Recommendations

ABSTRACT: The Davydov splitting of dye aggregates represents unique molecular excitons. In this paper, we report the formation of Davydov split aggregates of 3,3′-diethylthiacarbocyanine iodide ($DiSC_2$ (3)) and 3,3′-diethylthiadicarbocyanine iodide ($DiSC_2$ (5)) templated by the helical nanotubes of lithocholic acid (LCA). The templated Davydiv split aggregates show a strong J-band and a weak H-band in the adsorption spectra. As the LCA helical nanotubes transform into a straight shape, the relative intensities of the J-band and the H-band of the templated Davydov split aggregates become roughly equal. The twisted angle change of the transition moment of $DiSC_2$ (3) and $DiSC_2$ (5) molecules in the templated Davydov split aggregates in response to the helical-to-straight shape transformation of LCA nanotubes is estimated. The templated Dvaydov split aggregates with well-defined shapes and molecular excitons are of interest for artificial light-harvesting and optoelectronic devices.

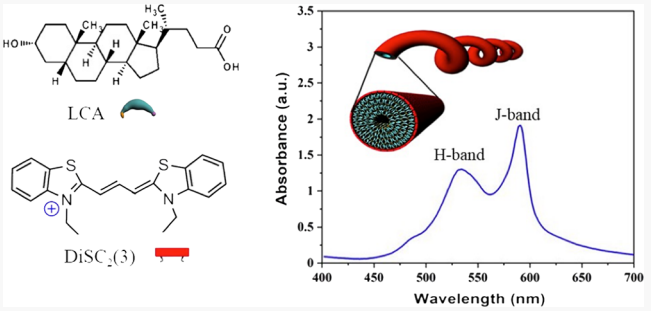

INTRODUCTION

The control of the aggregation of dyes through molecular assembly is a simple and powerful approach for designing functional nanomaterials.[1,2] It is known that the optical and excitonic properties of dyes strongly depend on their aggregate states. For J-aggregates, the transition dipole moments of dyes are parallel to each other in a head-to-tail arrangement. The arrangement only allows optical transitions to the lower excited state, giving rise to a red-shifted J-band with respect to the monomer band.[3] For H-aggregates, the transition dipole moments of dyes are parallel in a face-to-face arrangement. The arrangement only allows optical transitions to the higher excited state, showing a blue-shifted H-band compared with the monomer band. Oblique aggregates represent an intermediate arrangement between J- and H-aggregates, in which the transition dipole moments of dyes are twisted to each other. The twisted arrangement allows optical transitions to both the higher and lower excited states, consequently showing both the blue-shifted H-band and the red-shifted J-band in the absorption spectra, referred as to Davydov splitting.[4] Recently, there has been interest in the Davydov split aggregates of dyes because of their unique molecular excitons.[5−11]

Nature provides an excellent sample for precisely controlling the aggregation of chlorophylls by using proteins as a template in the assembly of highly efficient light-harvesting systems.[12] Cyanine dyes are an important conjugated molecule, which has been widely used in a variety of fields.[13] Inspired by the design of light-harvesting systems from nature, biopolymers including DNA,[14] peptides,[15,16] proteins,[17] amylose,[18] and hyaluronic acid[19] were used as templates for controlling the aggregation of cyanine dyes. However, it is a challenge to form the aggregates of cyanine dyes with well-defined sizes, shapes, and molecular excitons by using flexible biopolymers as templates since their conformations may change over time in solution. Recently, the helical nanoribbons from the co-assembly of gemini surfactants and enantiomeric tartrate counter ions were used as a rigid template for forming the H-aggregates of cyanine dyes with a narrow H-band and a remarkably large Stokes shift, in which the chirality of the helical nanoribbons was successfully transferred to the templated H-aggregates.[20]

Lithocholic acid (LCA) is a biological surfactant with several chiral centers, which can self-assemble into nanotubes in alkaline aqueous solution.[21−26] In this paper, we use the self-assembly of LCA in ammonia solution to form helical nanotubes. The adsorption behaviors of 3,3′-diethylthiacarbocyanine iodide ($DiSC_2$ (3)) and 3,3′-diethylthiadicarbocyanine iodide ($DiSC_2$ (5)) on the LCA helical nanotubes are studied. $DiSC_2$ (3) and $DiSC_2$ (5) adsorbed on the LCA helical nanotubes form Davydov split aggregates, showing a strong J-

Received: August 27, 2020
Revised: October 20, 2020
Published: November 4, 2020

https://dx.doi.org/10.1021/acs.langmuir.0c02537
Langmuir 2020, 36, 13649−13655

band and a weak H-band in the adsorption spectra. We find that the LCA helical nanotubes slowly transform into a straight shape after the adsorption of $DiSC_2$ (3) or $DiSC_2$ (5). The helical-to-straight transformation of LCA nanotubes causes the relative intensity change of the J- and H-bands of the templated Davydov split aggregates. The twisted angle change of the transition moments of $DiSC_2$ (3) and $DiSC_2$ (5) molecules in the templated Davydov split aggregates in response to the helical-to-straight shape transformation of LCA nanotubes is estimated.

EXPERIMENTAL SECTION

Materials. Lithocholic acid (LCA), 3,3′-diethylthiacarbocyanine iodide ($DiSC_2$ (3)), and 3,3′-diethylthiadicarbocyanine iodide ($DiSC_2$ (5)) were purchased from Sigma-Aldrich. They were used without further purification. Ammonia solution was from Sigma-Aldrich. Deionized water (18 MΩ cm, pH 5.7) was obtained from an Easypure II system. Holey Formvar films were obtained from SPI Supplies.

Formation of LCA Nanotubes. LCA was added into 15% ammonia solution in a glass vial to achieve a final concentration of 3 mM. LCA solution was sonicated in an ultrasonic bath (Branson 1510, Branson Ultrasonics Co.) at ∼50 °C for 5 min and then cooled to room temperature (23 °C). The translucent LCA solution in a sealed glass vial gradually turned into a milk-like solution over time as the self-assembly of LCA in ammonia solution progressed.

Adsorption of Cyanine Dyes on LCA Nanotubes. After the formation of LCA nanotubes in 15% ammonia solution, 0.2 mM $DiSC_2$ (3) or $DiSC_2$ (5) was added. The mixed solution was stirred for 2 min. After the adsorption of $DiSC_2$ (3) or $DiSC_2$ (5) at room temperature, LCA nanotubes were purified with centrifugation to remove excess $DiSC_2$ (3) or $DiSC_2$ (5) in solution.

Characterization. LCA nanotubes before and after the adsorption of $DiSC_2$ (3) or $DiSC_2$ (5) were imaged with scanning electron microscopy (SEM, Hitachi S3500N) and transmission electron microscopy (TEM, FEI Tecnai F30) conducted at 100 kV after being dried on holey Formvar films. ζ potential measurements of LCA nanotubes were carried with a Zetasizer Nano ZS90 (Malvern Instruments Inc.) at a cell driven voltage of 30 V. The adsorption of $DiSC_2$ (3) and $DiSC_2$ (5) on LCA nanotubes was characterized with a fluorescence microscope (Zeiss Axioscope-2 MOT), a Cary 400 UV–vis spectrophotometer, a JASCO FP-6500 spectrofluorometer, and a JASCO J-815 spectropolarimeter.

RESULTS AND DISCUSSION

The chemical structure of lithocholic acid (LCA) is shown in Figure 1a. LCA is a chiral molecule with several chiral centers. We found that the self-assembly of 3 mM LCA in 15% ammonia solution led to the formation of helical nanotubes after the LCA solution was aged at room temperature for 3 days (Figure 2a,b). The diameter of LCA helical nanotubes

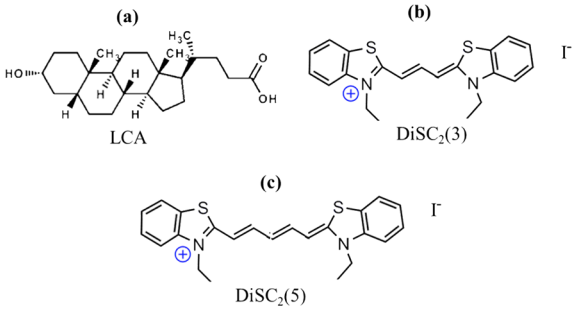

Figure 1. Chemical structures of lithocholic acid (LCA) (a), 3,3′-diethylthiacarbocyanine iodide ($DiSC_2$ (3)) (b), and 3,3′-diethylthiadicarbocyanine iodide ($DiSC_2$ (5)) (c).

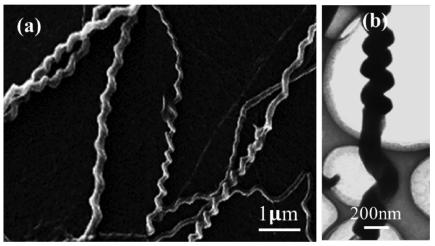

Figure 2. SEM (a) and TEM (b) images of self-assembled LCA nanotubes in 15% ammonia solution after being aged for 3 days at room temperature.

was measured to be 210 ± 20 nm. The twisted angle with respect to the long axis of helical nanotubes is in the range of 51 to 38°, and the pitch of helical nanotubes is 300 ± 50 nm. The twisting of LCA nanotubes suggests that the chirality of LCA is amplified to its supramolecular assemblies. Mesoscale simulations predicted that the final shape of supramolecular assemblies of chiral molecules was determined by the balance between elasticity and chirality.[27] The formation of LCA helical nanotubes suggests that the chiral interaction of LCA molecules provides sufficient energy to overcome the penalty of the elastic energy of LCA nanotubes and twists them into a helix. LCA has a carboxyl group linked to the steroid skeleton through a short alkyl chain (Figure 1a). The pK_a value of the carboxyl group of LCA in crystalline monolayers is 7.0−8.4.[28] The zeta potential of LCA helical nanotubes is −30.4 mV, suggesting that the LCA nanotubes are negatively charged due to the deprotonation of the carboxyl group of LCA in 15% ammonia solution.

The chemical structures of 3,3′-diethylthiacarbocyanine iodide ($DiSC_2$ (3)) and 3,3′-diethylthiadicarbocyanine iodide ($DiSC_2$ (5)) are shown in Figure 1b,c, respectively. They are cationic cyanine dyes. $DiSC_2$ (5) has a longer conjugated chain length than $DiSC_2$ (3). The monomer adsorption band is 556 nm for $DiSC_2$(3)[29] and 647 nm for $DiSC_2$(5).[30] As controlled experiments, we first studied the aggregation behaviors of $DiSC_2$ (3) and $DiSC_2$ (5) in 15% ammonia solution. 0.2 mM $DiSC_2$ (3) in 15% ammonia solution shows an absorption band at 555 nm (Figure 3a), which suggests that $DiSC_2$ (3) is in the monomer state. Meanwhile, 0.2 mM $DiSC_2$ (5) in 15% ammonia solution shows a sharp H-band at 549 nm, a monomer band at 647 nm, and a broad J-band with the maximum at 732 nm (Figure 3b). This result indicates that $DiSC_2$ (5) forms both H- and J-aggregates in 15% ammonia solution.

To study the interaction of $DiSC_2$ (3) with LCA helical nanotubes, we added 0.2 mM $DiSC_2$ (3) in the helical nanotube solution followed by stirring for 2 min. Figure 4a shows the fluorescence microscopy image of LCA helical nanotubes after 3 h of incubation with $DiSC_2$ (3) in 15% ammonia solution at room temperature, in which the helical nanotubes were excited at 550 nm. The fluorescence helical pattern shown in Figure 4a suggests that $DiSC_2$ (3) covers the entire length of LCA helical nanotubes. The adsorption of cationic $DiSC_2$ (3) on negatively charged LCA nanotubes is driven by electrostatic interaction. $DiSC_2$ (3) adsorbed on LCA helical nanotubes shows a strong J-band at 588 nm that is red-shifted with respect to the monomer band and a weak H-band at 545 nm that is blue-shifted with respect to the monomer band (Figure 4b). Since the J- and H-bands originate from the same aggregate templated by LCA helical

https://dx.doi.org/10.1021/acs.langmuir.0c02537
Langmuir 2020, 36, 13649−13655

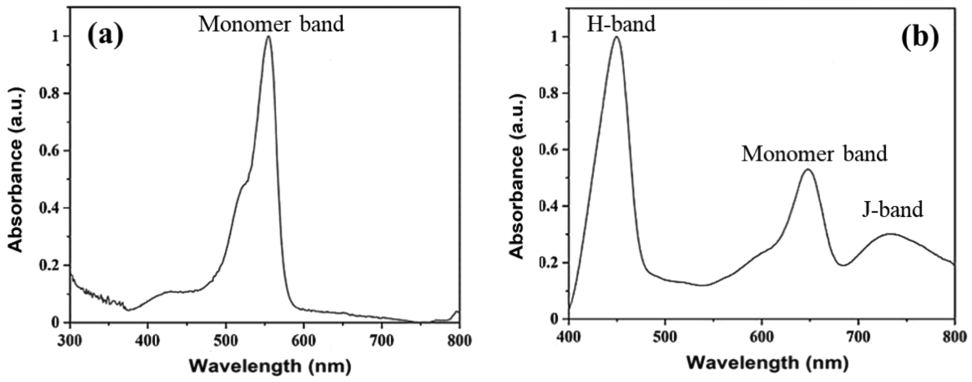

Figure 3. Adsorption spectra of 0.2 mM $DiSC_2$ (3) (a) and $DiSC_2$ (5) (b) in 15% ammonia solution after being aged for 3 days at room temperature.

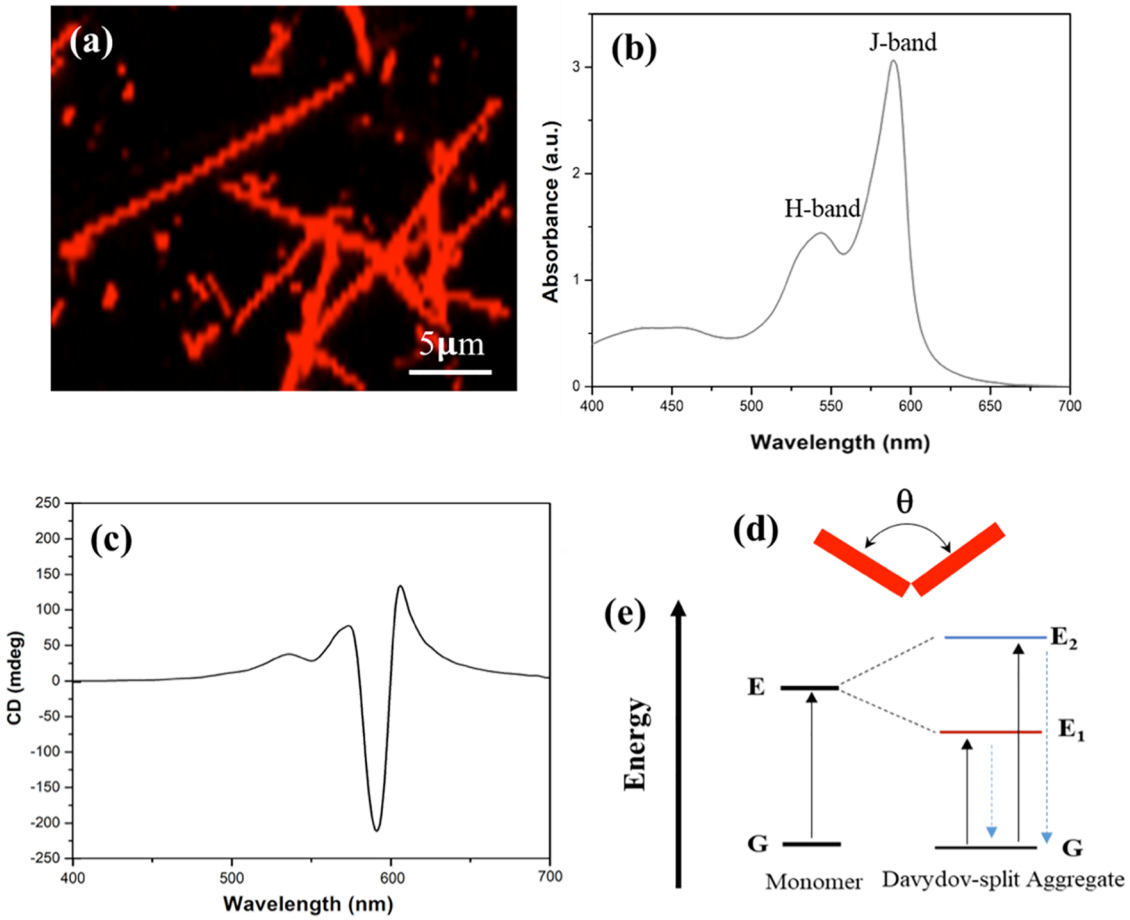

Figure 4. (a) Fluorescence microscopy image of LCA helical nanotubes after being incubated with $DiSC_2$ (3) for 3 h. Adsorption (b) and circular dichroism (c) spectra of $DiSC_2$ (3) adsorbed on LCA helical nanotubes after 3 h of incubation. (d) Schematic representation of a twisted arrangement of $DiSC_2$ (3) molecules in the templated Davydov split aggregates. (e) Energy level diagram of monomer and Davydov split aggregates. Absorption is represented by dark arrows, and emission is represented by blue arrows.

nanotubes, they should be related to each other. The Davydov splitting is an appropriate mechanism to explain the origin of both the J- and H-bands in the adsorption spectrum shown in Figure 4b. The Davydov splitting between the H-band and the J-band is asymmetric with respect to the monomer band (Figure 4b). The split of the J-band with respect to the monomer band is slightly larger than that of the H-band. The Davydov split aggregates of $DiSC_2$ (3) templated by LCA helical nanotubes are optically active, showing the strong circular dichroism (CD) signs in the J-band range and the weak CD signs in the H-band range (Figure 4c). The CD signs suggest the chiral arrangement of $DiSC_2$ (3) molecules in the templated Davydov split aggregates. Thus, we infer that the Davydov splitting is a result of the twisting of the transition moments of $DiSC_2$ (3) molecules to each other by an angle (θ) (Figure 4d). In this case, optical transitions to both the higher (E_2) and lower (E_1) excited states are possible (Figure 4e), giving rise to a blue-shifted H-band and a red-shifted J-band with respect to the monomer band.

https://dx.doi.org/10.1021/acs.langmuir.0c02537
Langmuir 2020, 36, 13649−13655

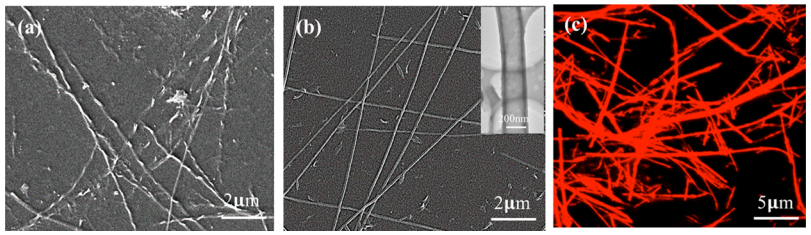

Figure 5. SEM images of LCA helical nanotubes after being incubated with $DiSC_2$ (3) in 15% ammonia solution for 24 (a) and 48 (b) h. (c) Fluorescence microscopy image of LCA straight nanotubes after being incubated with $DiSC_2$ (3) for 48 h. The inset in panel (b) shows the TEM image of a straight LCA nanotube.

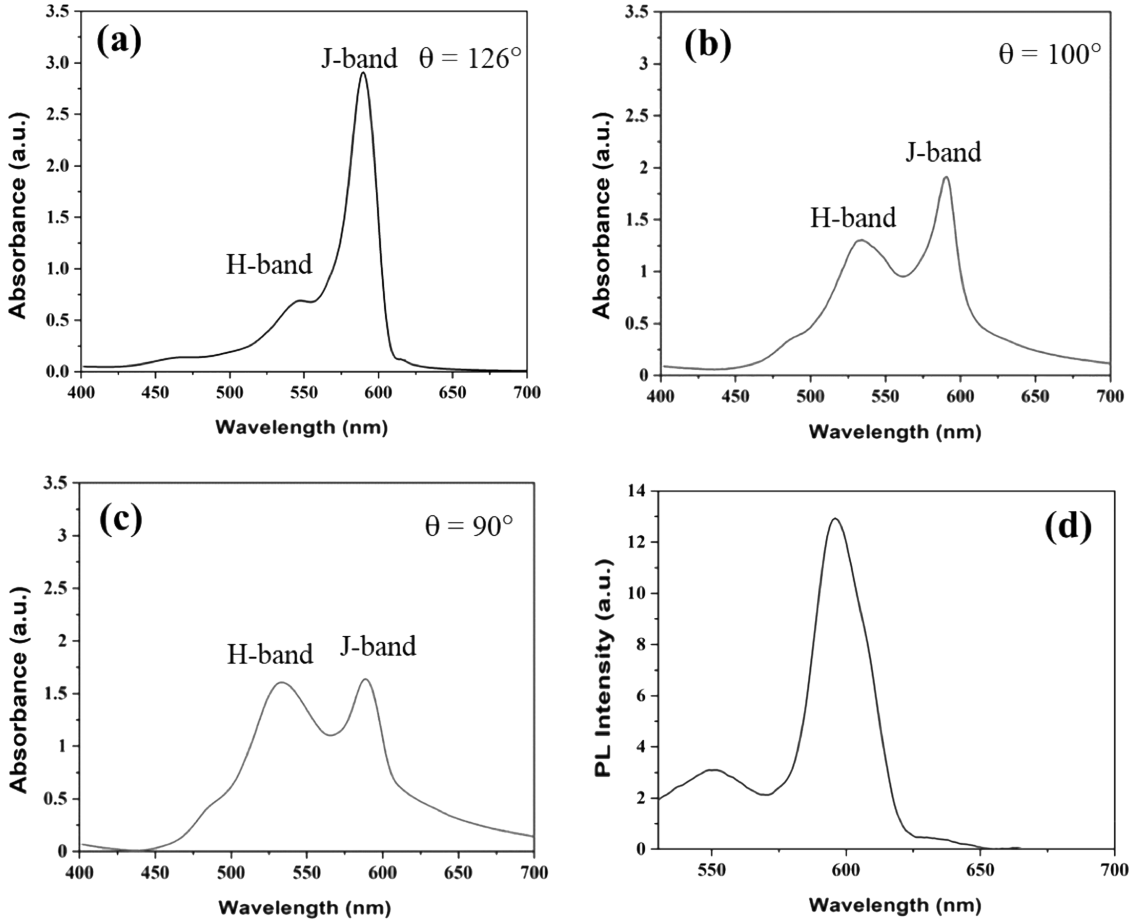

Figure 6. Adsorption spectra of $DiSC_2$ (3) after 1 (a), 24 (b), and 48 (c) h of incubation with LCA helical nanotubes in 15% ammonia solution at room temperature. (d) Fluorescence (FL) spectrum of $DiSC_2$ (3) adsorbed on LCA helical nanotubes after 48 h of incubation. The twisted angles (θ) of the transition moments of $DiSC_2$ (3), which was estimated from the adsorption spectra, are shown in panels (a–c).

Interestingly, the LCA helical nanotubes transform into a straight shape over time after the adsorption of $DiSC_2$ (3) (Figure 5a,b). The adsorption of $DiSC_2$ (3) is expected to strengthen the elastic energy of LCA nanotubes. Thus, the chiral interaction of LCA is unable to provide sufficient energy to overcome the penalty of the elastic energy of the LCA nanotubes with the Davydov split aggregate of $DiSC_2$ (3), leading to the helical-to-straight shape transition. After the helical-to-straight shape transformation, the hollowness of LCA nanotubes is easily observed (see the insert in Figure 5b). The uniform fluorescence signal along the entire length of LCA straight nanotubes confirms the adsorption of $DiSC_2$ (3) (Figure 5c). We find that the helical-to-straight shape transformation of LCA nanotubes causes the change of the adsorption spectrum of the templated Davydov split aggregate of $DiSC_2$ (3). As can be seen in Figure 6a–c, the intensity of the J-band decreases while the intensity of the H-band increases over time during the helical-to-straight shape transition of LCA nanotubes. However, there is no significant change in the splitting distance between the J- and H-bands. The relative intensities of the J- and H-bands of the Davydov split aggregates of $DiSC_2$ (3) on LCA straight nanotubes become roughly equal (Figure 6c). After being excited, the Davydov split aggregates of $DiSC_2$ (3) templated by LCA straight nanotubes show a weak fluorescence emission with a maximum at 550 nm that is slightly shifted with respect to the H-band (545 nm) and an intense fluorescence emission with a maximum at 592 nm that is slightly shifted with respect to the J-band (588 nm) (Figure 6d). The explanation of Davydov split aggregates is given in Figure 4e, in which the exciton band

https://dx.doi.org/10.1021/acs.langmuir.0c02537
Langmuir 2020, 36, 13649–13655

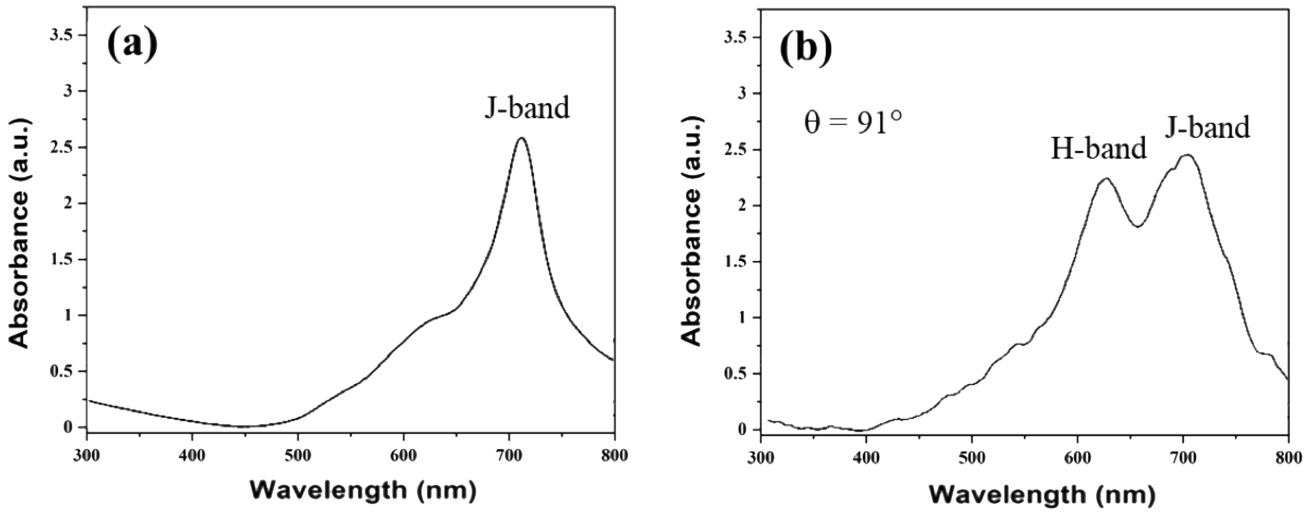

Figure 7. Adsorption spectra of $DiSC_2$ (5) after 1 (a) and 48 (c) h of incubation with LCA helical nanotubes in 15% ammonia solution at room temperature. The twisted angle (θ) of the transition moments of $DiSC_2$ (5), which was estimated from the adsorption spectra, is shown in panel (b).

splits into two energy states. The fluorescence emission at 550 nm arises from the higher energy state (E_2), while the fluorescence emission at 592 nm is from the lower energy state (E_1). It is clear from Figure 6d that the fluorescence emitted from the lower energy state is stronger than that from the higher energy state.

Furthermore, we studied the interaction of $DiSC_2$ (5) with LCA helical nanotubes. In our experiments, 0.2 mM $DiSC_2$ (5) was added into LCA helical nanotube solution. Figure 7a shows the adsorption spectrum of $DiSC_2$ (5) after 3 h of incubation with LCA helical nanotubes in 15% ammonia solution at room temperature. In 15% ammonia solution without LCA helical nanotubes, $DiSC_2$ (5) shows a sharp H-band at 549 nm and a broad J-band at 732 nm (Figure 3b). Meanwhile, $DiSC_2$ (5) adsorbed on LCA helical nanotubes shows a strong J-band at 706 nm that is red-shifted with respect to the monomer band at 647 nm and a shoulder at 620 nm. The shoulder grows into an H-band after the helical-to-straight shape transformation of LCA nanotubes (Figure 7b). In this case, the relative intensities of the H-band at 620 nm and the J-band at 706 nm of the templated Davydov split aggregates of $DiSC_2$ (5) are roughly equal. The Davydov splitting between the H-band and the J-band is asymmetric with respect to the monomer band. The Davydov splitting distance between the H-band and the J-band is 86 nm.

Our results clearly show that the shape of LCA nanotubes has a significant impact on the relative intensities of the J-band and the H-band of the templated Davydov split aggregates of $DiSC_2$ (3) and $DiSC_2$ (5). The relative intensities of the J-band and the H-band can be determined by the twisted angle (θ) of the transition moment of dye molecules in Davydov split aggregates:[31−33] $\tan^2\frac{\theta}{2} = \frac{A_{\text{J-band}}}{A_{\text{H-band}}}$, where $A_{\text{J-band}}$ and $A_{\text{H-band}}$ are the oscillation strengths of the J-band and the H-band, respectively. The ratio of $A_{\text{J-band}}/A_{\text{H-band}}$ is proportional to the ratio of the areas under the H-band and the J-band in the adsorption spectra. However, it is difficult to measure the area under the H-band and the J-band of the templated Davydov split aggregates of $DiSC_2$ (3) and $DiSC_2$ (5) because they show a certain degree of overlapping. In this case, we used the intensity ratio of the H-band and the J-band to replace the area ratio under the H-band and the J-band for roughly estimating the twisted angles (θ) of the transition moments of $DiSC_2$ (3) and $DiSC_2$ (5) molecules in the templated Davydov split aggregates.[31] The estimated angles (θ) of the transition moment of $DiSC_2$ (3) molecules from the adsorption spectra are inserted in Figure 6a−c. The twisted angle (θ) of the transition moment of $DiSC_2$ (3) molecules is ~90° in the Davydov split aggregates templated by LCA straight nanotubes and ~126° in the Davydov split aggregates templated by LCA helical nanotubes. Based on the relative intensities of the H-band and the J-band of the Davydov split aggregates of $DiSC_2$ (5) templated by LCA straight nanotubes (Figure 7b), the twisted angle (θ) of the transition moment of $DiSC_2$ (5) is estimated to be ~91°. These results are also in agreement with the predication of an essential states model, which was proposed for understanding the relative intensity change of the J-band and the H-band of the Davydov split aggregates of squaraine dimers.[34] The model predicted that the H-band was dominant when the twisted angle of the squaraine dimers was close to ~0°. The J-band becomes dominant when the twisted angle of the squaraine dimers was close to 180°. Both the J-band and the H-band were observed when the twisted angle of the squaraine dimers was in the range of 180 to 0°. The Davydov split aggregates of $DiSC_2$ (5) templated by LCA helical nanotubes are only characterized by a strong J-band (Figure 7a). Thus, we can infer that the twisted angle (θ) of the transition moment of $DiSC_2$ (5) should be close to 180°.

■ CONCLUSIONS

We have found that $DiSC_2$ (3) and $DiSC_2$ (5) adsorbed on self-assembled LCA nanotubes form Davydov split aggregates, showing both J- and H-bands in the adsorption spectra. The relative intensities of the J-band and the H-band depend on the shape of LCA nanotubes. On LCA helical nanotubes, the J-band of the templated Davydov split aggregates is dominant. On LCA straight nanotubes, the relative intensities of the J-band and the H-band of the templated Davydov split aggregates are roughly equal. From the adsorption spectra of the templated Davydov split aggregates, we estimate the twisted angle change of the transition moments of $DiSC_2$ (3) and $DiSC_2$ (5) in response to the helical-to-straight shape

https://dx.doi.org/10.1021/acs.langmuir.0c02537
Langmuir 2020, 36, 13649−13655

transformation of LCA nanotubes. Our results show that LCA nanotubes provide a unique template for designing the Dvaydov split aggregates with well-defined shapes and molecular excitons, which are potential for designing artificial light-harvesting and optoelectronic devices.

AUTHOR INFORMATION

Corresponding Author

Jiyu Fang − *Department of Materials Science and Engineering and Advanced Materials Processing and Analysis Center, University of Central Florida, Orlando, Florida 32816, United States*; Email: Jiyu.Fang@ucf.edu

Authors

Nitin Ramesh Reddy − *Department of Materials Science and Engineering and Advanced Materials Processing and Analysis Center, University of Central Florida, Orlando, Florida 32816, United States*

Samuel Rhodes − *Department of Materials Science and Engineering and Advanced Materials Processing and Analysis Center, University of Central Florida, Orlando, Florida 32816, United States*

Yiping Ma − *Department of Materials Science and Engineering and Advanced Materials Processing and Analysis Center, University of Central Florida, Orlando, Florida 32816, United States*

Complete contact information is available at: https://pubs.acs.org/10.1021/acs.langmuir.0c02537

Notes

The authors declare no competing financial interest.

ACKNOWLEDGMENTS

This work was supported by the US National Science Foundation (CBET 1803690).

REFERENCES

(1) Würthner, F.; Kaiser, T. E.; Saha-Möller, C. R. J-Aggregates: From Serendipitous Discovery to Supramolecular Engineering of Functional Dye Materials. *Angew. Chem., Int. Ed.* **2011**, *50*, 3376−3410.

(2) Spano, F. C. The Spectral Signatures of Frenkel Polarons in H- and J-aggregates. *Acc. Chem. Res.* **2010**, *43*, 429−439.

(3) Jelley, E. E. Spectral Absorption and Fluorescence of Dyes in the Molecular State. *Nature* **1936**, *138*, 1009−1010.

(4) Davydov, A. S. *Theory of Molecular Excitons*; Plenum press: New York, 1971.

(5) DeRossi, U.; Dahne, S.; Meskers, S. C. J.; Dekkers, H. P. J. M. Spontaneous Formation of Chirality in J-Aggregates Showing Davydov Splitting. *Angew. Chem., Int. Ed.* **1996**, *35*, 760−763.

(6) Pawlik, A.; Kirstein, S.; de Rossi, U.; Daehne, S. Structural Conditions for Spontaneous Generation of Optical Activity in J-Aggregates. *J. Phys. Chem. B* **1997**, *101*, 5646−5651.

(7) von Berlepsch, H.; Kirstein, S.; Bottcher, C. Controlling the Helicity of Tubular J-aggregates by Chiral Alcohols. *J. Phys. Chem. B* **2003**, *107*, 9646−9654.

(8) Vlaming, S. M.; Augulis, R.; Stuart, M. C. A.; Knoester, J.; van Loosdrecht, P. H. M. Exciton Spectra and the Microscopic Structure of Self-Assembled Porphyrin Nanotubes. *J. Phys. Chem. B* **2009**, *113*, 2273−2283.

(9) Pajusalu, M.; Raetsep, M.; Trinkunas, G.; Freiberg, A. Davydov Splitting of Excitons in Cyclic Bacteriochlorophyll a Nanoaggregates of Bacterial Light-Harvesting Complexes between 4.5 and 263 K. *ChemPhysChem* **2011**, *12*, 634−644.

(10) Yefimova, S. L.; Grygorova, G. V.; Klochkov, V. K.; Borovoy, I. A.; Sorokin, A. V.; Malyukin, Y. V. Molecular Arrangement in Cyanine Dye J-Aggregates Formed on CeO_2 Nanoparticles. *J. Phys. Chem. C* **2018**, *122*, 20996−21003.

(11) Cannon, B. L.; Patten, L. K.; Kellis, D. L.; Davis, P. H.; Lee, J.; Graugnard, E.; Yurke, B.; Knowlton, W. B. Large Davydov Splitting and Strong Fluorescence Suppression: An Investigation of Exciton Delocalization in DNA-Templated Holliday Junction Dye Aggregates. *J. Phys. Chem. A* **2018**, *122*, 2086−2095.

(12) Kühlbrandt, W.; Wang, D. N.; Fujiyoshi, Y. Atomic Model of Plant Light-Harvesting Complex by Electron Crystallography. *Nature* **1994**, *367*, 614−621.

(13) Mishra, A.; Behera, R. K.; Behera, P. K.; Mishra, B. K.; Behera, G. B. Cyanines During the 1990s: A Review. *Chem. Rev.* **2000**, *100*, 1973−2012.

(14) Wang, W.; Silva, G. L.; Armitage, B. A. DNA-Templated Formation of a Helical Cyanine Dye J-Aggregate. *J. Am. Chem. Soc.* **2000**, *122*, 9977−9986.

(15) Renikuntla, B. R.; Armitage, B. A. Role Reversal in a Supramolecular Assembly: A Chiral Cyanine Dye Controls the Helicity of a Peptide−Nucleic Acid Duplex. *Langmuir* **2005**, *21*, 5362−5366.

(16) Yang, Q.; Xiang, J.; Li, Q.; Yan, W.; Zhou, Q.; Tang, Y.; Xu, G. Chiral Transformation of Cyanine Dye Aggregates Induced by Small Peptides. *J. Phys. Chem. B* **2008**, *112*, 8783−8787.

(17) Zhang, Y.; Xiang, J.; Tang, Y.; Xu, G.; Yan, W. Chiral Transformation of Achiral J-aggregates of a Cyanine Dye Templated by Human Serum Albumin. *ChemPhysChem* **2007**, *8*, 224−226.

(18) Kim, O.-K.; Je, J.; Jernigan, G.; Buckley, L.; Whitten, D. Super-Helix Formation Induced by Cyanine J-Aggregates onto Random-Coil Carboxymethyl Amylose as Template. *J. Am. Chem. Soc.* **2006**, *128*, 510−516.

(19) Sagawa, T.; Tobata, H.; Ihara, H. Exciton Interactions in Cyanine Dye−Hyaluronic Acid (HA) Complex: Reversible and Biphasic Molecular Switching of Chromophores Induced by Random Coil-to-Double-Helix Phase Transition of HA. *Chem. Commun.* **2004**, *18*, 2090−2091.

(20) Ryu, N.; Okazaki, Y.; Pouget, E.; Takafuji, M.; Nagaoka, S.; Ihara, H.; Oda, R. Fluorescence Emission Originated from the H-aggregated Cyanine Dye with Chiral Gemini Surfactant Assemblies Having a Narrow Absorption Band and a Remarkably Large Stokes Shift. *Chem. Commun.* **2017**, *53*, 8870−8873.

(21) Terech, P.; Jean, B.; Ne, F. Hexagonally Ordered Ammonium Lithocholate Self-Assembled Nanotubes with Highly Monodisperse Solution. *Adv. Mater.* **2006**, *18*, 1571−1574.

(22) Pal, A.; Basit, H.; Sen, S.; Aswal, V. K.; Bhattacharya, S. Structure and Properties of Two component Hydrogels Comprising Lithocholic Acid and Organic Amines. *J. Mater. Chem.* **2009**, *19*, 4325−4334.

(23) Tamhane, K.; Zhang, X.; Zhou, J.; Fang, J. Assembly and Disassembly of Tubular Spherulites. *Soft Matter* **2010**, *6*, 1224−1228.

(24) Zhang, X.; Bera, T.; Liang, W.; Fang, J. Longitudinal Zipping/Unzipping of Self-Assembled Organic Tubes. *J. Phys. Chem. B* **2011**, *115*, 14445−14449.

(25) Terech, P.; Velu, S. K. P.; Pernot, P.; Wiegart, L. Salt Effects in the Formation of Self-Assembled Lithocholate Helical Ribbons and Tubes. *J. Phys. Chem. B* **2012**, *116*, 11344−11355.

(26) Wang, H.; Xu, W.; Song, S.; Feng, L.; Song, A.; Hao, J. Hydrogels Facilitated by Monovalent Cations and Their Use as Efficient Dye Adsorbents. *J. Phys. Chem. B* **2014**, *118*, 4693−4701.

(27) Selinger, R. L. B.; Selinger, J. V.; Malanoski, A. P.; Schnur, J. M. Shape Selection in Chiral Self-Assembly. *Phys. Rev. Lett.* **2004**, *93*, 158103.

(28) Leonard, M. R.; Bogle, M. A.; Carey, M. C.; Donovan, J. M. Spread Monomolecular Films of Monohydroxy Bile Acids and Their Salts: Influence of Hydroxyl Position, Bulk pH, and Association with Phosphatidylcholine. *Biochemistry* **2000**, *39*, 16064−16074.

(29) Rhodes, S.; Liang, W.; Shteinberg, E.; Fang, J. Formation of Spherulitic J-Aggregates from the Coassembly of Lithocholic Acid and Cyanine Dye. *J. Phys. Chem. Lett.* **2017**, *8*, 4504−4509.
(30) Reddy, N. R.; Rhodes, S.; Fang, J. Colorimetric Detection of Dopamine with J-Aggregate Nanotube-Integrated Hydrogel Thin Films. *ACS Omega* **2020**, *5*, 18198−18204.
(31) Saito, K.; Ikegami, K.; Kuroda, S. I.; Tabe, Y.; Sugi, M. Formation of Herringbone Structure with Davydov Splitting in Cyanine Dye-Adsorbed Langmuir Blodgett Films. *Jpn. J. Appl. Phys.* **1991**, *30*, 1836−1840.
(32) Kirstein, S.; Möhwald, H. Exciton Band Structures in 2D Aggregates of Cyanine Dyes. *Adv. Mater.* **1995**, *7*, 460−463.
(33) Tkacheva, T. N.; Yefimova, S. L.; Klochkov, V. K.; Borovoy, I. A.; Malyukin, Y. V. Spectroscopic Study of Ordered Hybrid Complexes Formation between Dye Aggregates and ReVO4:Eu3+(Re = Y, Gd, La) Nanoparticles. *J. Mol. Liq.* **2014**, *199*, 244−250.
(34) Zhong, C.; Bialas, D.; Collison, C. J.; Spano, F. C. Davydov Splitting in Squaraine Dimers. *J. Phys. Chem. C* **2019**, *123*, 18734−18745.

https://dx.doi.org/10.1021/acs.langmuir.0c02537
Langmuir 2020, 36, 13649−13655